



**HAL**  
open science

## Development and clinical validation of a simple and fast UPLC-ESI-MS/MS method for simultaneous quantification of nine kinase inhibitors and two antiandrogen drugs in human plasma: interest for their therapeutic drug monitoring

Benoit Llopis, Pascal Robidou, Nadine Tissot, Bruno Pinna, Paul Gougis, Fleur Cohen Aubart, Luca Campedel, Baptiste Abbar, Damien Roos-Weil, Madalina Uzunov, et al.

### ► To cite this version:

Benoit Llopis, Pascal Robidou, Nadine Tissot, Bruno Pinna, Paul Gougis, et al.. Development and clinical validation of a simple and fast UPLC-ESI-MS/MS method for simultaneous quantification of nine kinase inhibitors and two antiandrogen drugs in human plasma: interest for their therapeutic drug monitoring. *Journal of Pharmaceutical and Biomedical Analysis*, 2021, 197, pp.113968. 10.1016/j.jpba.2021.113968 . hal-03181430

**HAL Id: hal-03181430**

**<https://hal.sorbonne-universite.fr/hal-03181430v1>**

Submitted on 25 Mar 2021

**HAL** is a multi-disciplinary open access archive for the deposit and dissemination of scientific research documents, whether they are published or not. The documents may come from teaching and research institutions in France or abroad, or from public or private research centers.

L'archive ouverte pluridisciplinaire **HAL**, est destinée au dépôt et à la diffusion de documents scientifiques de niveau recherche, publiés ou non, émanant des établissements d'enseignement et de recherche français ou étrangers, des laboratoires publics ou privés.

1 **Development and clinical validation of a simple and fast UPLC-ESI-MS/MS method for**  
2 **simultaneous quantification of nine kinase inhibitors and two antiandrogen drugs in**  
3 **human plasma: interest for their therapeutic drug monitoring.**

4

5 Benoit Llopis 1, Pascal Robidou 1, Nadine Tissot 1, Bruno Pinna 1, Paul Gougis 1,2, Fleur  
6 Cohen Aubart 3, Luca Campedel 2, Baptiste Abbar 1, Damien Roos Weil 4, Madalina  
7 Uzunov 4, Joseph Gligorov 5, Joe-Elie Salem 1, Christian Funck-Brentano 1, Noël Zahr 1

8

9 1. AP-HP.Sorbonne Université, Department of Pharmacology and Clinical Investigation  
10 Center (CIC-1901), Pitié-Salpêtrière Hospital; INSERM, CIC-1901 and UMR-S 1166,  
11 Sorbonne Université, Faculty of Medicine Sorbonne Université, Faculty of Medicine,Paris,  
12 France.

13 2. AP-HP Sorbonne Université, Pitié-Salpêtrière Hospital, institut universitaire de  
14 cancérologie, département d'oncologie médicale, CLIP2 Galilée Paris, France

15 3. AP-HP Sorbonne Université, Pitié-Salpêtrière Hospital, Service de Médecine Interne 2,  
16 Centre National de Référence Maladies Systémiques Rares et Histiocytoses, Paris, France

17 4. AP-HP Sorbonne Université, Service d'Hématologie Clinique, Pitié-Salpêtrière Hospital,  
18 Paris, France.

19 5. Institut Universitaire de Cancérologie. AP-HP Sorbonne Université, INSERM U-938,  
20 CLIP(2) Galilée, Tenon Hospital, Medical Oncology Department, Paris, France.

21

22 Corresponding Author

23 Dr Noël Zahr,

24 Service de Pharmacologie

25 Hôpital Pitié-Salpêtrière, APHP, 75013 Paris, France

26 Tel: + 33 1 42 16 20 15, Fax: +33 1 42 16 20 46

27 Email: [noel.zahr@aphp.fr](mailto:noel.zahr@aphp.fr)

28

29

30

31

32 **Abstract**

33 Kinase inhibitors (KIs) and antiandrogen drugs (AAs) are oral anticancer drugs with narrow  
34 therapeutic index that exhibit high inter- and intra-individual variability. We describe here a  
35 UPLC-MS/MS method for the simultaneous quantification of nine KIs: cobimetinib,  
36 dasatinib, ibrutinib, imatinib, nilotinib, palbociclib, ruxolitinib, sorafenib and vemurafenib;  
37 two active metabolites of them: N-desmethyl imatinib, N-oxide sorafenib; and two AAs:  
38 abiraterone and enzalutamide; with short pre-treatment and run time in order to be easily used  
39 in clinical practice for their therapeutic drug monitoring (TDM) and facilitating  
40 pharmacokinetics and pharmacokinetics/pharmacodynamics studies. Plasma samples were  
41 prepared by a single-step protein precipitation. Analytes were separated on a Waters Acquity  
42 UPLC<sup>®</sup> T3 HSS C18 column by non-linear gradient elution; with subsequent detection by  
43 Xevo<sup>®</sup> TQD triple quadrupole tandem mass spectrometer in a positive ionization mode.  
44 Analysis time was 2.8 minutes per run, and all analytes eluted within 1.46-1.97 minutes. The  
45 analytical performance of the method in terms of specificity, sensitivity, linearity, precision,  
46 accuracy, matrix effect, extraction recovery, limit of quantification, dilution integrity and  
47 stability of analytes under different conditions met all criteria for a bioanalytical method for  
48 the quantification of drugs. The calibration curves were linear over the range of 1-500 ng/mL  
49 for abiraterone, dasatinib and ibrutinib; 5-500 ng/mL for cobimetinib and palbociclib; 10-  
50 5,000 ng/mL for imatinib, N-desmethyl imatinib, nilotinib, sorafenib, N-oxide sorafenib and  
51 ruxolitinib; 100-50,000 ng/mL for enzalutamide and 100-100,000 ng/mL for vemurafenib  
52 with coefficient of correlation above 0.995 for all analytes. This novel method was  
53 successfully applied to TDM in clinical practice.

54

55 Keywords: liquid chromatography, mass spectrometry, therapeutic drug monitoring, kinase  
56 inhibitors, antiandrogens, oral targeted therapies.

## 57 **1. Introduction**

58 Kinase inhibitors (KIs) such as: cobimetinib, dasatinib, ibrutinib, imatinib, nilotinib,  
59 palbociclib, ruxolitinib, sorafenib and vemurafenib; and antiandrogen drugs (AAs) such as:  
60 abiraterone acetate and enzalutamide; both belonging to the class of oral targeted therapies  
61 characterized by high specificity for single or multiple key biological pathways responsible or  
62 implicated in the cancer process.

63 KIs target molecular aberrations of cancer cells by blocking intracellular signals driving  
64 proliferation in malignant cells [1]. They have an important activity on many types of kinases  
65 (tyrosine or serine/threonine) involved in tumour growth, angiogenesis, and metastatic  
66 progression of cancer [2]. KIs, analysed in this study, are used for treating various  
67 haematological malignancies: dasatinib, ibrutinib, imatinib, nilotinib; and solid tumours  
68 including gastrointestinal stromal tumours: imatinib; advanced renal cell carcinoma:  
69 sorafenib; breast cancer: palbociclib; hepatocellular carcinoma: sorafenib; melanoma and  
70 erdheim-chester disease: vemurafenib and cobimetinib [3]. Furthermore, ruxolitinib have been  
71 approved for use in the treatment of myelofibrosis and graft versus host disease.

72 Abiraterone acetate and enzalutamide are both oral antiandrogen drugs approved for treatment  
73 of metastatic prostate cancer. Both drugs inhibit tumour growth effects of androgens.

74 Abiraterone inhibits the production of adrenal androgens, whereas enzalutamide functions as  
75 an androgen receptor signalling inhibitor [4].

76 Oral administration of these drugs is associated with a better quality of life but patients  
77 prescribed oral therapies struggle with adherence [3]. Moreover, these molecules display large  
78 pharmacokinetics (PK) variability. Indeed, they are metabolized mostly by cytochromes P450  
79 3A4 [5], whose activity is known to present a large inter-individual variability and to be  
80 influenced by environmental factors such as food or drug-induced interactions [6]. Likewise,  
81 inherent factors such as age, gender, medical conditions or genetics contribute to this

82 variability [3]. A given dose can therefore yield very different exposure levels, favouring the  
83 selection of resistant cellular clones in case of sub-therapeutic drug exposure or increasing the  
84 risk of adverse reactions at excessive plasma levels. Targets, cancers indication and potential  
85 effect of food and drug-drug interaction in their PK are summarized in Table 1 for each drug  
86 analysed in this study.

87 In parallel with this PK variability, some of these drugs display an exposure-response  
88 relationship [7]. For example; sorafenib, palbociclib and imatinib show an exposure-toxicity  
89 relationship [8–10]. Similarly; abiraterone, enzalutamide, vemurafenib and dasatinib show an  
90 exposure-efficacy relationship [11–13]. Furthermore, cardiovascular toxicities associated with  
91 most of these latter drugs have an exposure-toxicity relationship yet to be explored [14–17].

92 The poor adherence, the PK variability and the pharmacokinetics/pharmacodynamics  
93 (PK/PD) relationship of these molecules suggest the potential interest of their therapeutic drug  
94 monitoring (TDM) [3]. It has been established that the therapeutic use of targeted anticancer  
95 drugs could be optimized by an individualization of their dosage, based on plasma  
96 concentrations measurement. Target concentrations as well as efficacy and/or toxicity  
97 thresholds have been proposed for some molecules although there is currently no consensus  
98 [7].

99 We describe here a rapid, selective, sensitive and simple UPLC-MS/MS method for the  
100 simultaneous analysis, in small volume of plasma, of nine KIs: cobimetinib, dasatinib,  
101 ibrutinib, imatinib, nilotinib, palbociclib, ruxolitinib, sorafenib and vemurafenib; two of their  
102 active metabolites: N-desmethyl imatinib, N-oxide sorafenib; and two AAs: abiraterone and  
103 enzalutamide to enable their TDM and support PK studies and research protocols for  
104 molecule for which PK/PD relationship needs to be characterized.

105

106

## 107 2. Materials and methods

108

### 109 2.1. Chemical and reagents

110 Abiraterone (ABIRA), enzalutamide (ENZA), ibrutinib (IBRU), imatinib (IMA), nilotinib  
111 (NILO), N-oxide sorafenib (NO-SORA), palbociclib (PALBO), ruxolitinib (RUXO),  
112 sorafenib (SORA), [<sup>2</sup>H<sub>4</sub>]-abiraterone (d4-ABIRA), [<sup>13</sup>C<sub>6</sub>]-cobimetinib (<sup>13</sup>C<sub>6</sub>-COBI), [<sup>2</sup>H<sub>5</sub>]-  
113 ibrutinib (d5-IBRU), [<sup>2</sup>H<sub>8</sub>]-imatinib (d8-IMA), [<sup>13</sup>C,<sup>2</sup>H<sub>3</sub>]-nilotinib (d3-NILO), [<sup>2</sup>H<sub>3</sub>]-N-oxide  
114 sorafenib (d3-NO-SORA), [<sup>2</sup>H<sub>8</sub>]-palbociclib (d8-PALBO), [<sup>2</sup>H<sub>9</sub>]-ruxolitinib (d9-RUXO) and  
115 [<sup>13</sup>C,<sup>2</sup>H<sub>3</sub>]-sorafenib (d3-SORA) were purchased from Alsachim<sup>®</sup> (Illkrich, France) while  
116 cobimetinib (COBI), dasatinib (DASA), N-desmethyl imatinib (DM-IMA), vemurafenib  
117 (VEMU), [<sup>2</sup>H<sub>8</sub>]-dasatinib (d8-DASA) and [<sup>2</sup>H<sub>6</sub>]-vemurafenib (d6-VEMU) were purchased  
118 from LGC<sup>®</sup> (Augsburg, Germany). The chemical structures of analytes (except metabolites)  
119 are shown in Figure 1. Methanol and dimethylsulfoxide (DMSO) were obtained from Merck<sup>®</sup>  
120 (Darmstadt, Germany). Formic acid and ammonium acetate were obtained from Sigma-  
121 Aldrich<sup>®</sup> (Munich, Germany). Zinc sulphate heptahydrate (ZnSO<sub>4</sub>\*7H<sub>2</sub>O) was obtained from  
122 VWR<sup>®</sup> (Fontenay-sous-Bois, France). All reagents used were of the highest available  
123 analytical grades. Liquid chromatography–MS/MS grade water was purchased from a water  
124 distribution hypergrade system Purelab Flex<sup>®</sup> (ELGA<sup>®</sup>), and drug-free plasma (blank plasma)  
125 from healthy donors was supplied by the French Blood Establishment (Paris, France).

### 126 2.2. Preparation of stock solutions, standards and quality control samples

127 Individual stock solutions of each analyte were prepared at 1 mg/mL. Stock solutions of  
128 ABIRA, COBI, DASA, ENZA, IBRU, IMA, DM-IMA, NILO, NO-SORA, RUXO, SORA  
129 and VEMU were prepared in DMSO, while stock solution of PALBO was prepared in  
130 hydrochloric acid 0.1M. Working solutions, obtained by diluting the stock solutions with  
131 methanol, were prepared for each analyte. Calibration standard and quality control (QC)

132 samples were prepared in blank human plasma by spiking with an appropriate volume of each  
133 working solutions. The ranges of the different analytes covered in the current method are: 1-  
134 500 ng/mL (1-5-10-50-100-250-500) for ABIRA, DASA and IBRU; 5-500 ng/mL (5-10-50-  
135 100-250-500) for COBI and PALBO; 10-5,000 ng/mL (10-50-100-500-1,000-2,500-5,000)  
136 for IMA, DM-IMA, NILO, NO-SORA, SORA and RUXO; 100-50,000 ng/mL (100-500-  
137 2,000-10,000-20,000-50,000) for ENZA and 100-100,000 ng/mL (100-500-2,000-10,000-  
138 20,000-50,000-100,000) for VEMU. The QC samples were tested at four different  
139 concentrations: high QC (HQC: 80% of upper limit of quantification), medium QC (MQC:  
140 50% of selected range), low QC (LQC: 2-10 times the LLOQ) and QC at LLOQ. Individual  
141 stock solutions of each isotopic internal standard (IS) were prepared in adequate solvent at 1  
142 mg/mL. A solution of mix of each IS (ISmix) at 15 ng/mL for d4-ABIRA, d5-IBRU, d6-  
143 PALBO, d8-DASA and <sup>13</sup>C<sub>6</sub>-COBI; 150 ng/mL for d5-SORA, d3-NILO, d3-NO-SORA, d6-  
144 RUXO and d8-IMA; and 1,500 ng/mL for d6-ENZA and d6-VEMU was prepared in  
145 methanol. As DM-IMA and IMA display very close chemical structures and a similar  
146 chromatographic behaviour, d8-IMA was used as IS for both compounds. All stock solutions,  
147 working solutions, calibration standards, ISmix and QC samples were stored at -20°C.

148

### 149 2.3. Instruments and analytical conditions

150 Chromatography was performed on an Acquity UPLC<sup>®</sup> system (WATERS<sup>®</sup>, Milford,  
151 Massachusetts, United States) with an autosampler temperature at 10°C. Acquity UPLC<sup>®</sup> T3  
152 HSS C18 analytical column (2.1 x 100 mm, 1.8 µm particle size) was used for  
153 chromatographic separation and column temperature was maintained at 45°C. The mobile  
154 phase had a flow rate of 0.4 mL/min with a non-linear gradient elution and the run time  
155 analysis was set at 2.8 min. The UPLC system was coupled to a triple quadrupole mass  
156 spectrometer: Xevo<sup>®</sup> TQD (WATERS<sup>®</sup>, Milford, Massachusetts, United States).

157 Quantifications were achieved in Multiple Reactions Monitoring (MRM) mode and  
158 electrospray ionization was operated in positive mode (ESI+) for each analyte. The source  
159 temperature and the desolvation temperature were set at 150°C and 380°C, respectively, with  
160 a desolvation gas flow of 800 L/h and a cone gas flow of 30 L/h. The capillary voltage was set  
161 at 3.0 kV. Argon was used as collision gas with a flow set at 0.22 mL/min. Chromatographic  
162 data acquisition; peak integration and quantification were performed using MassLynx® 4.2  
163 software.

#### 164 2.4. Samples pre-treatment

165 Sample preparation was performed by single-step protein precipitation: 100 µL of aqueous  
166 ZnSO<sub>4</sub>\*7H<sub>2</sub>O (10%, w/v; pH 5.40) and 200 µL of ISmix were added to 50 µL of human  
167 plasma, calibrator or QC samples. The mixture was vortexed for 1 min using a MixMate®  
168 Vortex Mixer (Eppendorf®, Sydney, Australia) and centrifuged for 10 min at 18,900 g using a  
169 Heraeus Biofuge Primo® centrifuge (Thermo Fisher Scientific®, Massachusetts, United  
170 States). Finally, the supernatant was transferred to a Waters Acquity® autosampler vial and 10  
171 µL were injected into the LC-MS/MS system using a temperature-controlled autosampler  
172 device at 10°C.

#### 173 2.5. Method validation

174 The validation was performed according to European Medicines Agency (EMA) guidelines  
175 and US Food and Drug Administration (FDA) guidelines for the validation of bioanalytical  
176 methods. Parameters included were selectivity, carry-over, linearity, accuracy and precision,  
177 lower limit of quantification, matrix effect, extraction recovery, stability in human plasma and  
178 dilution integrity.

##### 179 2.5.1. Selectivity

180 Six different sources of plasma samples were tested. A selective method should not have



181 interference of more than 20% of the lower limit of quantification (LLOQ) of the analyte.

182

### 183 2.5.2. Carry-over

184 As our method is designed to measure very low and very high concentrations simultaneously,  
185 a carry-over test was performed. Carry-over was assessed by injecting blank samples after a  
186 high concentration calibrator. Carry-over in the blank sample following the high  
187 concentration calibrator should not be greater than 20% of the LLOQ of the analyte.

### 188 2.5.3. Linearity

189 Calibration curves were acquired by plotting the peak area ratio of the concentration of each  
190 analyte standard to the area of their respective isotopic IS (except for DM-IMA analyzed with  
191 d8-IMA) over the range from 1-500 ng/mL for ABIRA, DASA and IBRU; 5-500 ng/mL for  
192 COBI and PALBO; 10-5,000 ng/mL for IMA, DM-IMA, NILO, NO-SORA, RUXO and  
193 SORA; 100-50,000 ng/mL for ENZA and 100-100,000 ng/mL for VEMU. Each curve was  
194 assayed by least square weighted (1/x). Linearity was defined by a coefficient of correlation  $r$   
195  $\geq 0.995$ .

### 196 2.5.4. Precision and accuracy

197 The intra-day precision and accuracy were evaluated using 6 different replicates, extracted in  
198 the same day, of QC samples at the four concentrations (LLOQ, LQC, MQC and HQC).

199 The inter-day precision and accuracy were determined by extracting each QC sample (LLOQ,  
200 LQC, MQC and HQC) 6 times a day over 3 different days ( $n = 18$  replicates). The  
201 concentration of each QC levels was determined using calibration standards prepared on the  
202 same day. The precision was calculated as the coefficient of variation (CV, %) within a single  
203 run (intra-day assay) and between different runs (inter-day assay), and the accuracy as the  
204 percentage ratio of the measured and nominal concentration (mean of measured/nominal  $\times$

205 100). The acceptance limits were CV<15% for precision and within  $\pm 15\%$  of the nominal  
206 concentration for accuracy (range from 85-115%).

207

#### 208 2.5.5. Lower limit of quantification

209 The lower limit of quantification (LLOQ) for analytes in human plasma samples was defined  
210 as the lowest concentration detectable with a signal-to-noise ratio of at least 10, CV<20% and  
211 accuracy of 80-120%. For each analyte, the LLOQ was selected as the lower concentration  
212 covered by the selected range.

213

#### 214 2.5.6. Matrix effect and extraction recovery

215 Matrix effect (ME) and extraction recovery (ER) were assessed at three QC levels (LQC,  
216 MQC and HQC) in quintuplicate (with five different sources of plasma) for each analytes.  
217 The approach involves determination of ratio of peak areas of analyte in three different sets,  
218 one consisting of analyte standards in methanol (set A), one prepared in blank matrix extracts  
219 and spiked after extraction (set B), and one prepared in blank matrix from the same sources  
220 but spiked before extraction (set C). ME and ER were calculated by the following equations:  
221  $ME (\%) = B/A*100$  and  $ER (\%) = C/B*100$ . A value above or below 100% for the ME  
222 indicates an ionization enhancement or suppression, respectively. ME was considered  
223 negligible for a ratio ranging from 85-115% and CV<15%; ER ranging from 85-115% and  
224 CV<15% showing good efficiency of the method.

#### 225 2.5.7. Stability

226 The stability of the analytes in plasma was tested by comparing accuracy and precision of  
227 three QC levels (LQC, MQC and HQC) kept under different storage conditions using freshly  
228 prepared calibrators. The stability of analytes was tested immediately after samples  
229 preparation (baseline) and after four conditions: short-term storage at 25°C (72h), short-term

230 storage at 4°C (1 week), long-term storage at -20°C (8 weeks) and after three cycles of freeze  
231 and thaw. In this later condition, samples stored for a minimum of 12h at -20°C, were kept at  
232 room temperature for at least 30min followed by freezing in -20°C for a minimum of 12h.  
233 The concentrations obtained after these different storage conditions were compared with the  
234 baseline concentration of each QC levels. All stability tests were done in quintuplicate per QC  
235 level. For each analytes, it was considered to be stable in plasma when measured  
236 concentration within  $\pm 15\%$  of the baseline concentration. Stability of extracts kept onboard  
237 the autosampler at 10°C during 48h was also tested.

#### 238 2.5.8. Dilution integrity

239 The dilution integrity was examined to ascertain that an unknown sample with concentration  
240 exceeding the upper limit of compounds calibration range, could be diluted with blank matrix  
241 without influencing the accuracy and precision of the measurement. To achieve this, a sample  
242 was prepared at higher concentration (1,000 ng/mL for ABIRA, COBI, DASA, PALBO and  
243 IBRU; and 10,000 ng/mL for IMA, DM-IMA, NILO, NO-SORA, SORA and RUXO)  
244 followed by dilution (1:3) in blank plasma before extraction. Diluted sample was done in  
245 quintuplicate. The accuracy and precision of the diluted sample was not to deviate by more  
246 than 15%. We did not perform the test for ENZA and VEMU because it is unlikely that  
247 concentrations greater than 50,000 and 100,000 ng/mL, respectively, would be found in  
248 clinical practice.

249

#### 250 2.6. Clinical application

251 This UPLC-MS/MS quantification method was applied to measurement of oral targeted  
252 therapies in plasma of patients. Peripheral venous blood samples were taken as part of the  
253 routine clinical care from adult cancer patients treated with oral targeted therapies to perform

254 TDM. Blood samples were collected into lithium heparin tubes before taking the drugs  
255 ( $C_{\text{trough}}$ ) at steady state. Based on their reported  $T_{\text{max}}$ , blood samples were also collected at 1h  
256 or 3 h after taking the drug ( $C_{\text{max}}$ ) for RUXO and DASA, respectively, because the peak  
257 concentration are associated with clinical efficacy for both drugs. For IBRU, three successive  
258 samples were collected: at  $C_{\text{trough}}$  and 2h ( $C_{\text{max}}$ ) + 4h after taking the drug (concentration in  
259 the elimination phase) to determine area under the curve (AUC). AUC was derived from  
260 plasma concentration–time data by noncompartmental method using Phoenix WinNonLin®  
261 4.1 software (Certara, St. Louis, Missouri).  $AUC_{0-24h}$  was estimated considering that, at steady  
262 state, the concentration found 24h after taking the drug was equal to the  $C_{\text{trough}}$ . Plasma  
263 samples were prepared by centrifuging collected blood samples for 5 min at 4,500 g. All  
264 plasma samples were frozen at  $-20^{\circ}\text{C}$  until analysis, and were processed and analysed as  
265 described above. French regulations on non-interventional observational studies do not  
266 require patient’s consent when analyzing data obtained from routine care. Approval for data  
267 collection was obtained from the Commission Nationale de l’Informatique et des Libertés  
268 (n°1491960v0).

269

### 270 3. Results

271

#### 272 3.1. Optimization of LC-MS/MS conditions

273 Electrospray positive mode yielded a better spectrometer response than the negative mode. To  
274 achieve symmetrical peak shapes, good resolution and a short chromatographic run time, a  
275 mobile phase consisting of (A) water-formic acid (100:0.1, v/v)-ammonium acetate 2 mM  
276 ( $\text{pH}^* 2.82$ ) and (B) methanol-formic acid (100:0.1, v/v)-ammonium acetate 2 mM ( $\text{pH}^* 4.30$ )  
277 was used in the experiments using non-linear gradient elution. Mass spectrometry parameters  
278 for the LC-MS/MS determination of each analyte and their respective IS are shown in Table  
279 2.

## 280 3.2. Sample pre-treatment

281 Tandem mass spectrometry is sufficiently selective and sensitive to allow a simple and fast  
282 pre-treatment procedure as described. The efficiency of the pre-treatment was evident from  
283 high extraction recovery values and minimized matrix effects.

## 284 3.3. Method validation

285

### 286 3.3.1. Selectivity and carry-over

287 Six different sources of plasma samples without analytes but containing the following drugs:  
288 voriconazole, posaconazole, topiramate, diazepam, levetiracetam, lacosamide, clonazepam,  
289 lansoprazole, paracetamol, tramadol, furosemide, ceftriaxone, levofloxacin, rifampicin and  
290 amoxicillin were tested. These drugs were tested due to their relatively common use and for  
291 their possible concomitant administration in our cohort of patients. No interference with  
292 endogenous compounds or tested drugs was observed above 20% of the LLOQ of the analytes  
293 and with the same transitions and retention times of the studied analytes or their respective  
294 isotopic IS. All analytes and ISs were eluted within 1.45-1.97 min. The retention time of each  
295 analyte are shown in Table 2. The carry-over observed with the different analytes was less  
296 than 20% of the LLOQ [ABIRA (1.2%), COBI (0.8%), DASA (2%), ENZA (1.8%), IBRU  
297 (0.3%), IMA (0.5%), DM-IMA (0.2%), NILO (0.7%), NO-SORA (1.3%), PALBO (3.2%),  
298 RUXO (2.1%), SORA (0.7%) and VEMU (1.3%)]. Furthermore, no carry over was observed  
299 for any of the IS used.

### 300 3.3.2. Linearity

301 Calibration curves were linear with coefficient of correlation greater than  $r = 0.9972$  for all  
302 analytes (ranged from 0.9972 to 0.9999). All calibrators, analyzed on seven different days,  
303 were measured with an accuracy ranged from 88-112% and coefficient of variation less than  
304 11.6%. The linear regression equations of each analyte are shown in Table 2.

### 305 3.3.3. Accuracy and precision

306 Intra- and inter-day precision and accuracy outcomes of QC samples are shown in Table 3 and  
307 Table 4, respectively. The intra- and inter-day coefficients of variation ranged from 0.8% to  
308 9.4% and from 1.4% to 12.3% respectively, for all analytes at all tested concentrations (LQC,  
309 MQC and HQC). Likewise, the inter-day accuracy ranged from 89-110%, for all the analytes  
310 at all tested concentrations (LQC, MQC and HQC).

### 311 3.3.4. Lower limit of quantification

312 The LLOQ was established at 1 ng/mL for ABIRA, DASA and IBRU; 5 ng/mL for COBI and  
313 PALBO; 10 ng/mL for IMA, DM-IMA, NILO, NO-SORA, SORA and RUXO; and at 100  
314 ng/mL for ENZA and VEMU (Table 3 and 4). The chromatogram of the different analytes at  
315 their LLOQ is shown in Figure 2.

### 316 3.3.5. Matrix effect and extraction recovery

317 Matrix effect and extraction recovery for all the analytes ranged from 87-122% and 76-113%,  
318 respectively, and were stable over the concentration range for each of them, as shown in Table  
319 5. The result of matrix effect indicated that there was no significant ionization suppression or  
320 maximization resulting from sample matrices. Moreover, the method resulted in high recovery  
321 value at all QCs showing good efficiency except for abiraterone (Table 5). Abiraterone  
322 showed relative low recovery in this experiment. However, this relative low recovery did not  
323 interfere significantly with the quantitative determination of abiraterone concentration in  
324 plasma, as judged by linearity, accuracy and precision.

### 325 3.3.6. Stability

326 Table 5 shows the stability of each analyte in plasma. All analytes were stable in plasma at  
327 25°C up to 72h, except for IBRU for which degradation was observed after 24h. For IBRU,

328 we dosed each QC level, stored at 25°C, every hour for 8 consecutive hours to precisely  
329 establish the length of stability at room temperature. No degradation was observed during 8h.  
330 Therefore, IBRU degrades between 8-24h at room temperature. All analytes, except for  
331 ibrutinib, were stable in plasma at 4°C up to 1 week. Plasma stability of ibrutinib was  
332 demonstrated at 4°C up to 48h. Likewise, all analytes were stable in plasma at -20°C up to 8  
333 weeks. Regarding freeze and thaw stability, all analytes were stable after three freeze and  
334 thaw cycles. Furthermore, after extraction, the extracts were stable for at least 48h when kept  
335 onboard the autosampler at 10°C.

#### 336 3.3.7. Dilution integrity

337 The accuracy (% true) and precision (% CV) of the diluted samples were: ABIRA (98; 2.9),  
338 COBI (96; 3.1), DASA (100; 4.3), IBRU (95; 5.2), IMA (98; 1.6), DM-IMA (103; 3.6), NILO  
339 (100; 1.3), NO-SORA (105; 1.9), PALBO (98; 2.3), RUXO (101; 1.2) and SORA (110; 2.1).

340

#### 341 3.4. Clinical application

342 This validated UPLC-MS/MS method was successfully applied to the TDM of eighty adult  
343 patients with various haematological malignancies, prostate cancer, graft versus host disease,  
344 renal carcinoma or Erdheim-Chester disease and treated with oral targeted therapies,  
345 especially ibrutinib, dasatinib, imatinib, nilotinib, sorafenib, abiraterone, enzalutamide,  
346 ruxolitinib, vemurafenib and cobimetinib which are the most frequently required as part of  
347 TDM in our hospital. The analytes were easily detected and measured in patients' plasma.  
348 The results are summarized in Table 6. Moreover, as shown in Figure 3, no interferences were  
349 observed between the studied targeted therapies and endogenous compounds or others drugs  
350 given to participating cancer patients.

351

#### 352 4. Discussion

353 We describe here a method for the simultaneous quantification of nine KIs (cobimetinib,  
354 dasatinib, ibrutinib, imatinib, nilotinib, palbociclib, ruxolitinib, sorafenib and vemurafenib),  
355 and two AAs (abiraterone and enzalutamide). We specifically chose these molecules to meet  
356 the request of clinicians and because most of them have an exposure-response relationship  
357 well studied [8–13] for which an established or accepted target concentration exists [7].  
358 Furthermore, cardiovascular toxicities associated with ibrutinib, abiraterone and enzalutamide  
359 have been demonstrated by our team [14–17] and this method will allow us to explore the  
360 possible exposure-cardiovascular toxicities relationship with these drugs.

361 Each KI generates an important number of metabolites that are often inactive. However,  
362 sorafenib and imatinib have active metabolites: N-oxide sorafenib and N-desmethyl imatinib,  
363 respectively, which seems relevant to quantify.

364 Based on the high recovery, relative low intra- and inter-day CVs, and good linearity, the  
365 present method is suitable for detection and quantification of each analyte in human plasma.

366 Several LC-MS/MS analytical methods have been published to quantify one or more KI but  
367 few methods quantify up to 9 KIs. Van Dyk et al. [18] described a simultaneous quantification  
368 of 18 KIs in human plasma including dasatinib, ibrutinib, imatinib, nilotinib, ruxolitinib,  
369 sorafenib and vemurafenib. Likewise, Andriamanana et al. [19] described the simultaneous  
370 analysis of 9 KIs including dasatinib, imatinib, nilotinib and sorafenib; whereas Huynh et al.  
371 [20] described a method for quantification of 14 KIs including cobimetinib, dasatinib,  
372 ibrutinib, imatinib, nilotinib, sorafenib and vemurafenib. In these three methods, the authors  
373 did not quantify the active metabolites of imatinib and sorafenib, while some studies suggest  
374 their importance for TDM. The AUC (N-oxide SORA) and the ratio [AUC (N-oxide  
375 SORA)/AUC (SORA)] seems to be reliable predictors of adverse effects [21]. Likewise, a



376 correlation between imatinib + N-desmethyl imatinib exposure and hematologic toxicity were  
377 showed [10]. Janssen et al. [22] have also developed a method for the quantification of 9 KIs  
378 in human plasma including only cobimetinib and palbociclib. The authors thus made a choice  
379 different from ours on the selection of the molecules to be measured. Finally, Merienne et al.  
380 [23] and Bouchet et al. [24] reported a technique quantifying 17 and 9 KIs, respectively,  
381 including dasatinib, imatinib and its metabolite, nilotinib, ruxolitinib and sorafenib but using a  
382 solid-phase extraction procedure more complex than the protein precipitation extraction used  
383 in our method. The method we developed was designed to perform therapeutic monitoring of  
384 these drugs in a routine setting. This requires that our method should be simple, fast and  
385 practical. The stringent workup for preparation of calibration and QCs plasma samples  
386 containing thirteen different analytes is counterbalanced by a simplified extraction step.

387 Likewise, several LC-MS/MS analytical methods have been published to quantify one or  
388 more AAs. Van Nuland et al. [25] described a method for simultaneous quantification of  
389 abiraterone, enzalutamide and their major metabolites in human plasma and Kim et al. [26]  
390 reported a method for simultaneous quantification of abiraterone, enzalutamide, N-desmethyl  
391 enzalutamide and bicalutamide. Both methods allow quantification of active metabolites of  
392 abiraterone and enzalutamide unlike our method. However both methods focus only on  
393 antiandrogen drugs. Furthermore, some studies suggest that these metabolites (N-desmethyl  
394 enzalutamide and  $\Delta(4)$ -abiraterone) are unlikely to have meaningful contribution to the  
395 pharmacodynamics activity of abiraterone and enzalutamide. No exposure-response  
396 relationship was found in the PK/PD studies, which does not support the need for the  
397 monitoring of their plasma concentration in clinical practice [27,28].

398 Finally, there are many methods in the literature for the measurement of KIs or AAs but to  
399 our knowledge, neither combined both. Our method is the first that allows simultaneous  
400 quantification of 9 KIs, 2 metabolites of them and 2 AAs in human plasma. The measurement

401 of all these drugs in a single run is advantageous in light of the possible combined use of  
402 multiple KIs in future clinical practice. Indeed, several trials using combinations of KIs are  
403 listed on the United States clinical trials registration site: for example nilotinib/imatinib in  
404 gastrointestinal stromal tumours, chronic myeloid leukemia and Ph<sup>+</sup>/Bcr-Abl<sup>+</sup> acute  
405 lymphoblastic leukemia (NCT01089595, NCT01819389), ruxolitinib/dasatinib or nilotinib in  
406 chronic myeloid leukemia (NCT03654768), cobimetinib/vemurafenib in melanoma  
407 (NCT02537600, NCT03224208). Similar to melanoma, combination approaches using  
408 cobimetinib/vemurafenib have been used successfully in Erdheim-Chester disease [29]. In  
409 addition, there is some potential for the KI/AA combination in future clinical practice: Hongxi  
410 Wu et al. [30] demonstrated in their study that sorafenib therapy improved the efficacy of  
411 enzalutamide in the castration-resistant prostate cancer (CRPC) model, indicating a promising  
412 therapeutic strategy for clinical CRPC patients, and a phase I/II study of enzalutamide with  
413 and without sorafenib in advanced hepatocellular carcinoma patients is in progress  
414 (NCT02642913). The abiraterone/dasatinib combination in men with mCRPC are also been  
415 tested [31]. Moreover, our method is one of the few to quantify palbociclib in human plasma  
416 using mass spectrometry detection. Only five recent papers describe methods for the  
417 quantification of palbociclib in human plasma using LC-MS/MS [22,32–35] while the  
418 existence of a exposure-toxicity relationship is possible [9].

419 Concerning the selected ranges of concentrations tested, the LLOQ of analytes was lower in  
420 some methods compared with those we used. This can be explained by the fact that their  
421 plasma volume, and their injection volume into the LC-MS/MS system were higher as  
422 compared to those we used (50  $\mu$ L and 10  $\mu$ L respectively). Furthermore, this parameter  
423 depends on the sensitivity of the mass spectrometer used. We estimated that it was not  
424 necessary to improve this parameter since our LLOQs are already under the measured  
425 concentration in most patients. Likewise, none of the patients' samples were measured above

426 the ULOQs. In addition, in case of concentrations exceeding our ULOQs, the dilution  
427 integrity test shows that the sample can be diluted in blank plasma without affecting analyte  
428 response and assay precision or accuracy. This new method has large concentration range  
429 which makes it suitable for the measurement of the maximum and minimum concentrations  
430 reported for all studied drugs and is therefore applicable to TDM.

431 In most published methods, the volume of plasma samples and run time analysis varies from  
432 50-300  $\mu\text{L}$ , and 5-15 min, respectively [18–20,22–26,32]. Our method is rapid with fast  
433 sample preparation and run times (2.8 min) and requires only a small volume of plasma (50  
434  $\mu\text{L}$ ), which could reduce the time required for quantification of large number of samples and  
435 the blood volume collected from the patients. In the method of Jolibois et al. [33] the run time  
436 was 2.5 min but the volume of plasma samples was 150  $\mu\text{L}$ . In contrast, the volume of plasma  
437 samples was 10  $\mu\text{L}$  but the run time was 6.5 min in the method of Posocco et al. [34].  
438 Furthermore, with respect to other methods, our method is the one of the few in which each  
439 analyte (except for N-desmethyl Imatinib) are analyzed with respect to their respective  
440 isotopic internal standard.

441 Concerning stability, we found that ibrutinib should be dispatched to the laboratory without  
442 delay due to instability at room temperature. Huynh et al. [20] showed in their study that  
443 ibrutinib was stable in plasma for at least 4h at room temperature. We showed that this was  
444 the case for at least 8h. This may be important in order to manage shipping of samples coming  
445 from other hospitals. Likewise, all analytes were stable for at least 2 months at  $-20^{\circ}\text{C}$  in  
446 plasma. This is particularly important for clinical research protocols, where samples may need  
447 to be stored for a long time before they can be assayed.

448 Finally, the first clinical experience with the method confirms its suitability for clinical  
449 application (Table 6). We are currently working to incorporate 18 additional KIs (afatinib,  
450 alectinib, axitinib, bosutinib, brigatinib, cabozantinib, capmatinib, crizotinib, dabrafenib,

451 erlotinib, gefitinib, lenvatinib, osimertinib, pazopanib, ponatinib, ribociclib, trametinib,  
452 vandetanib) in order to be able to quantify most kinase inhibitors used in clinical practice to  
453 provide a TDM platform for oral targeted therapies.

454

## 455 **5. Conclusion**

456 We have developed and validated a rapid, sensitive, selective, accurate, precise and reliable  
457 UPLC-MS/MS method for the simultaneous quantification of nine kinase inhibitors, two of  
458 their active metabolites and two antiandrogen drugs in human plasma. This method is  
459 currently used in clinical practice for TDM of oral targeted therapies for which an established  
460 or accepted target concentration exists. In the future, this method could be adapted to  
461 incorporate additional KIs and AAs for which PK/PD relationship needs to be studied.

462

463

464

465

466

467

468

469

470

471

472 **Credit authorship contribution statement**

473 **Benoit Llopis:** Conceptualization, Validation, Visualization, Writing - original draft, Writing  
474 – review & editing

475 **Pascal Robidou:** Technical realization, review & editing

476 **Nadine Tissot:** Investigation, review & editing

477 **Bruno Pinna:** Investigation, review & editing

478 **Paul Gougis:** Investigation, review & editing

479 **Luca Campedel:** Investigation, review & editing

480 **Fleur Cohen Aubart:** Investigation, review & editing

481 **Baptiste Abbar:** Investigation, review & editing

482 **Damien Roos Weil:** Investigation, review & editing

483 **Madalina Uzunov:** Investigation, review & editing

484 **Joseph Gligorov:** Investigation, review & editing

485 **Joe-Elie Salem:** Investigation, review & editing

486 **Christian Funck-Brentano:** Investigation, Supervision, Writing – review & editing

487 **Noël Zahr:** Conceptualization, Validation, Supervision, Writing – review & editing

488

489 **Declaration of Competing Interest**

490 The authors declare that they have no known competing financial interests or personal  
491 relationships that could have appeared to influence the work reported in this paper.

492

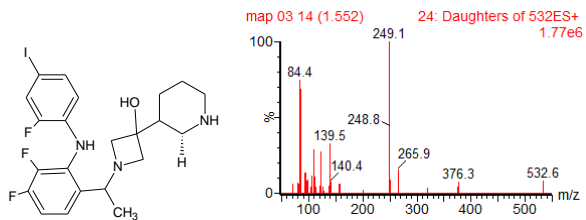
493 **References**

- 494 [1] N.A. Cohen, T.S. Kim, R.P. DeMatteo, Principles of Kinase Inhibitor Therapy for Solid Tumors,  
 495 *Ann. Surg.* 265 (2017) 311–319. <https://doi.org/10.1097/SLA.0000000000001740>.
- 496 [2] M. Jeltsch, V.-M. Leppänen, P. Saharinen, K. Alitalo, Receptor Tyrosine Kinase-Mediated  
 497 Angiogenesis, *Cold Spring Harb. Perspect. Biol.* 5 (2013).  
 498 <https://doi.org/10.1101/cshperspect.a009183>.
- 499 [3] P. Gougis, L.-J. Palmieri, C. Funck-Brentano, A. Paci, R. Flippot, O. Mir, R. Coriat, Major pitfalls of  
 500 protein kinase inhibitors prescription: A review of their clinical pharmacology for daily use, *Crit.*  
 501 *Rev. Oncol. Hematol.* 141 (2019) 112–124. <https://doi.org/10.1016/j.critrevonc.2019.06.006>.
- 502 [4] M. Barber, L.S. Nguyen, J. Wassermann, J.-P. Spano, C. Funck-Brentano, J.-E. Salem, Cardiac  
 503 arrhythmia considerations of hormone cancer therapies, *Cardiovasc. Res.* 115 (2019) 878–894.  
 504 <https://doi.org/10.1093/cvr/cvz020>.
- 505 [5] K.T. Kivistö, H.K. Kroemer, M. Eichelbaum, The role of human cytochrome P450 enzymes in the  
 506 metabolism of anticancer agents: implications for drug interactions., *Br. J. Clin. Pharmacol.* 40  
 507 (1995) 523–530.
- 508 [6] Y.L. Teo, H.K. Ho, A. Chan, Metabolism-related pharmacokinetic drug–drug interactions with  
 509 tyrosine kinase inhibitors: current understanding, challenges and recommendations, *Br. J. Clin.*  
 510 *Pharmacol.* 79 (2015) 241–253. <https://doi.org/10.1111/bcp.12496>.
- 511 [7] A. Mueller-Schoell, S.L. Groenland, O. Scherf-Clavel, M. van Dyk, W. Huisinga, R. Michelet, U.  
 512 Jaehde, N. Steeghs, A.D.R. Huitema, C. Kloft, Therapeutic drug monitoring of oral targeted  
 513 antineoplastic drugs, *Eur. J. Clin. Pharmacol.* (2020). [https://doi.org/10.1007/s00228-020-](https://doi.org/10.1007/s00228-020-03014-8)  
 514 [03014-8](https://doi.org/10.1007/s00228-020-03014-8).
- 515 [8] P. Boudou-Rouquette, C. Narjoz, J.L. Golmard, A. Thomas-Schoemann, O. Mir, F. Taieb, J.-P.  
 516 Durand, R. Coriat, A. Dauphin, M. Vidal, M. Tod, M.-A. Lorient, F. Goldwasser, B. Blanchet, Early  
 517 sorafenib-induced toxicity is associated with drug exposure and UGT1A9 genetic polymorphism  
 518 in patients with solid tumors: a preliminary study, *PLoS One.* 7 (2012) e42875.  
 519 <https://doi.org/10.1371/journal.pone.0042875>.
- 520 [9] W. Sun, P.J. O’Dwyer, R.S. Finn, A. Ruiz-Garcia, G.I. Shapiro, G.K. Schwartz, A. DeMichele, D.  
 521 Wang, Characterization of Neutropenia in Advanced Cancer Patients Following Palbociclib  
 522 Treatment Using a Population Pharmacokinetic-Pharmacodynamic Modeling and Simulation  
 523 Approach, *J. Clin. Pharmacol.* 57 (2017) 1159–1173. <https://doi.org/10.1002/jcph.902>.
- 524 [10] C. Delbaldo, E. Chatelut, M. Ré, A. Deroussent, S. Séronie-Vivien, A. Jambu, P. Berthaud, A. Le  
 525 Cesne, J.-Y. Blay, G. Vassal, Pharmacokinetic-pharmacodynamic relationships of imatinib and its  
 526 main metabolite in patients with advanced gastrointestinal stromal tumors, *Clin. Cancer Res.*  
 527 *Off. J. Am. Assoc. Cancer Res.* 12 (2006) 6073–6078. [https://doi.org/10.1158/1078-0432.CCR-](https://doi.org/10.1158/1078-0432.CCR-05-2596)  
 528 [05-2596](https://doi.org/10.1158/1078-0432.CCR-05-2596).
- 529 [11] X. Wang, A. Roy, A. Hochhaus, H.M. Kantarjian, T.-T. Chen, N.P. Shah, Differential effects of  
 530 dosing regimen on the safety and efficacy of dasatinib: retrospective exposure-response  
 531 analysis of a Phase III study, *Clin. Pharmacol. Adv. Appl.* 5 (2013) 85–97.  
 532 <https://doi.org/10.2147/CPAA.S42796>.
- 533 [12] G.E. Benoist, R.J. Hendriks, P.F.A. Mulders, W.R. Gerritsen, D.M. Somford, J.A. Schalken, I.M.  
 534 van Oort, D.M. Burger, N.P. van Erp, Pharmacokinetic Aspects of the Two Novel Oral Drugs  
 535 Used for Metastatic Castration-Resistant Prostate Cancer: Abiraterone Acetate and  
 536 Enzalutamide, *Clin. Pharmacokinet.* 55 (2016) 1369–1380. [https://doi.org/10.1007/s40262-016-](https://doi.org/10.1007/s40262-016-0403-6)  
 537 [0403-6](https://doi.org/10.1007/s40262-016-0403-6).
- 538 [13] E. Funck-Brentano, J.C. Alvarez, C. Longvert, E. Abe, A. Beauchet, C. Funck-Brentano, P. Saiag,  
 539 Plasma vemurafenib concentrations in advanced BRAFV600mut melanoma patients: impact on  
 540 tumour response and tolerance, *Ann. Oncol. Off. J. Eur. Soc. Med. Oncol.* 26 (2015) 1470–1475.  
 541 <https://doi.org/10.1093/annonc/mdv189>.
- 542 [14] J.-E. Salem, A. Manouchehri, M. Bretagne, B. Lebrun-Vignes, J.D. Groarke, D.B. Johnson, T. Yang,  
 543 N.M. Reddy, C. Funck-Brentano, J.R. Brown, D.M. Roden, J.J. Moslehi, Cardiovascular Toxicities

- 544 Associated With Ibrutinib, *J. Am. Coll. Cardiol.* 74 (2019) 1667–1678.  
 545 <https://doi.org/10.1016/j.jacc.2019.07.056>.
- 546 [15] J.E. Salem, T. Yang, J.J. Moslehi, X. Waintraub, E. Gandjbakhch, A. Bachelot, F. Hidden-Lucet, J.S.  
 547 Hulot, B.C. Knollmann, B. Lebrun-Vignes, C. Funck-Brentano, A.M. Glazer, D.M. Roden,  
 548 Androgenic effects on ventricular repolarization: A translational study from the international  
 549 pharmacovigilance database to iPSC-cardiomyocytes, *Ann. Endocrinol.* (2020).  
 550 <https://doi.org/10.1016/j.ando.2020.02.008>.
- 551 [16] J. Alexandre, J.J. Moslehi, K.R. Bersell, C. Funck-Brentano, D.M. Roden, J.-E. Salem, Anticancer  
 552 drug-induced cardiac rhythm disorders: Current knowledge and basic underlying mechanisms,  
 553 *Pharmacol. Ther.* 189 (2018) 89–103. <https://doi.org/10.1016/j.pharmthera.2018.04.009>.
- 554 [17] M. Bretagne, B. Lebrun-Vignes, A. Pariente, C.M. Shaffer, G.G. Malouf, P. Dureau, C. Potey, C.  
 555 Funck-Brentano, D.M. Roden, J.J. Moslehi, J.-E. Salem, Heart failure and atrial tachyarrhythmia  
 556 on abiraterone: A pharmacovigilance study, *Arch. Cardiovasc. Dis.* 113 (2020) 9–21.  
 557 <https://doi.org/10.1016/j.acvd.2019.09.006>.
- 558 [18] M. van Dyk, J.O. Miners, G. Kichenadasse, R.A. McKinnon, A. Rowland, A novel approach for the  
 559 simultaneous quantification of 18 small molecule kinase inhibitors in human plasma: A platform  
 560 for optimised KI dosing, *J. Chromatogr. B Analyt. Technol. Biomed. Life. Sci.* 1033–1034 (2016)  
 561 17–26. <https://doi.org/10.1016/j.jchromb.2016.07.046>.
- 562 [19] I. Andriamanana, I. Gana, B. Duret, A. Hulin, Simultaneous analysis of anticancer agents  
 563 bortezomib, imatinib, nilotinib, dasatinib, erlotinib, lapatinib, sorafenib, sunitinib and  
 564 vandetanib in human plasma using LC/MS/MS, *J. Chromatogr. B Analyt. Technol. Biomed. Life.  
 565 Sci.* 926 (2013) 83–91. <https://doi.org/10.1016/j.jchromb.2013.01.037>.
- 566 [20] H.H. Huynh, C. Pressiat, H. Sauvageon, I. Madelaine, P. Maslanka, C. Lebbé, C. Thieblemont, L.  
 567 Goldwirt, S. Mourah, Development and Validation of a Simultaneous Quantification Method of  
 568 14 Tyrosine Kinase Inhibitors in Human Plasma Using LC-MS/MS, *Ther. Drug Monit.* 39 (2017)  
 569 43–54. <https://doi.org/10.1097/FTD.0000000000000357>.
- 570 [21] M. Shimada, H. Okawa, Y. Kondo, T. Maejima, Y. Kataoka, K. Hisamichi, M. Maekawa, M.  
 571 Matsuura, Y. Jin, M. Mori, H. Suzuki, T. Shimosegawa, N. Mano, Monitoring Serum Levels of  
 572 Sorafenib and Its N-Oxide Is Essential for Long-Term Sorafenib Treatment of Patients with  
 573 Hepatocellular Carcinoma, *Tohoku J. Exp. Med.* 237 (2015) 173–182.  
 574 <https://doi.org/10.1620/tjem.237.173>.
- 575 [22] J.M. Janssen, N. de Vries, N. Venekamp, H. Rosing, A.D.R. Huitema, J.H. Beijnen, Development  
 576 and validation of a liquid chromatography-tandem mass spectrometry assay for nine oral  
 577 anticancer drugs in human plasma, *J. Pharm. Biomed. Anal.* 174 (2019) 561–566.  
 578 <https://doi.org/10.1016/j.jpba.2019.06.034>.
- 579 [23] C. Merienne, M. Rousset, D. Ducint, N. Castaing, K. Titier, M. Molimard, S. Bouchet, High  
 580 throughput routine determination of 17 tyrosine kinase inhibitors by LC–MS/MS, *J. Pharm.  
 581 Biomed. Anal.* 150 (2018) 112–120. <https://doi.org/10.1016/j.jpba.2017.11.060>.
- 582 [24] S. Bouchet, E. Chauzit, D. Ducint, N. Castaing, M. Canal-Raffin, N. Moore, K. Titier, M. Molimard,  
 583 Simultaneous determination of nine tyrosine kinase inhibitors by 96-well solid-phase extraction  
 584 and ultra performance LC/MS-MS, *Clin. Chim. Acta Int. J. Clin. Chem.* 412 (2011) 1060–1067.  
 585 <https://doi.org/10.1016/j.cca.2011.02.023>.
- 586 [25] M. van Nuland, M.J.X. Hillebrand, H. Rosing, J.H.M. Schellens, J.H. Beijnen, Development and  
 587 Validation of an LC-MS/MS Method for the Simultaneous Quantification of Abiraterone,  
 588 Enzalutamide, and Their Major Metabolites in Human Plasma, *Ther. Drug Monit.* 39 (2017)  
 589 243–251. <https://doi.org/10.1097/FTD.0000000000000387>.
- 590 [26] K. Kim, R.A. Parise, J.L. Holleran, L.D. Lewis, L. Appleman, N. van Erp, M.J. Morris, J.H. Beumer,  
 591 Simultaneous quantitation of abiraterone, enzalutamide, N-desmethyl enzalutamide, and  
 592 bicalutamide in human plasma by LC-MS/MS, *J. Pharm. Biomed. Anal.* 138 (2017) 197–205.  
 593 <https://doi.org/10.1016/j.jpba.2017.02.018>.
- 594 [27] M.-L. Joulia, E. Carton, A. Jouinot, M. Allard, O. Huillard, N. Khoudour, M. Peyromaure, M.  
 595 Zerbib, A.T. Schoemann, M. Vidal, F. Goldwasser, J. Alexandre, B. Blanchet,

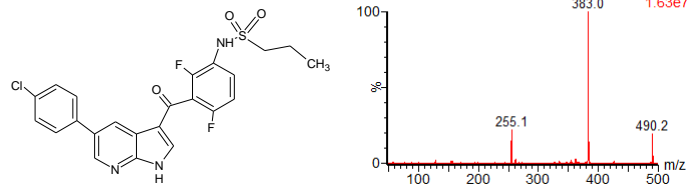
- 596 Pharmacokinetic/Pharmacodynamic Relationship of Enzalutamide and Its Active Metabolite N-  
 597 Desmethyl Enzalutamide in Metastatic Castration-Resistant Prostate Cancer Patients, *Clin.*  
 598 *Genitourin. Cancer.* (2019). <https://doi.org/10.1016/j.clgc.2019.05.020>.
- 599 [28] M. van Nuland, S.L. Groenland, A.M. Bergman, N. Steeghs, H. Rosing, N. Venekamp, A.D.R.  
 600 Huitema, J.H. Beijnen, Exposure–response analyses of abiraterone and its metabolites in real-  
 601 world patients with metastatic castration-resistant prostate cancer, *Prostate Cancer Prostatic*  
 602 *Dis.* 23 (2020) 244–251. <https://doi.org/10.1038/s41391-019-0179-5>.
- 603 [29] G. Goyal, M.L. Heaney, M. Collin, F. Cohen-Aubart, A. Vaglio, B.H. Durham, O. Hershkovitz-  
 604 Rokah, M. Girschikofsky, E.D. Jacobsen, K. Toyama, A.M. Goodman, P. Hendrie, X. Cao, J.I.  
 605 Estrada-Veras, O. Shpilberg, A. Abdo, M. Kurokawa, L. Dagna, K.L. McClain, R.D. Mazor, J.  
 606 Picarsic, F. Janku, R.S. Go, J. Haroche, E.L. Diamond, Erdheim-Chester disease: consensus  
 607 recommendations for evaluation, diagnosis, and treatment in the molecular era, *Blood.* 135  
 608 (2020) 1929–1945. <https://doi.org/10.1182/blood.2019003507>.
- 609 [30] H. Wu, L. Zhang, X. Gao, X. Zhang, J. Duan, L. You, Y. Cheng, J. Bian, Q. Zhu, Y. Yang,  
 610 Combination of sorafenib and enzalutamide as a potential new approach for the treatment of  
 611 castration-resistant prostate cancer, *Cancer Lett.* 385 (2017) 108–116.  
 612 <https://doi.org/10.1016/j.canlet.2016.10.036>.
- 613 [31] N. Spetsieris, M. Boukovala, J.A. Weldon, A. Tsikkinis, A. Hoang, A. Aparicio, S.-M. Tu, J.C.  
 614 Araujo, A.J. Zurita, P.G. Corn, L. Pagliaro, J. Kim, J. Wang, S.K. Subudhi, N.M. Tannir, C.J.  
 615 Logothetis, P. Troncoso, X. Wang, S. Wen, E. Efstathiou, A Phase 2 Trial of Abiraterone Followed  
 616 by Randomization to Addition of Dasatinib or Sunitinib in Men With Metastatic Castration-  
 617 Resistant Prostate Cancer, *Clin. Genitourin. Cancer.* (2020).  
 618 <https://doi.org/10.1016/j.clgc.2020.05.013>.
- 619 [32] A. Martínez-Chávez, H. Rosing, M. Hillebrand, M. Tibben, A.H. Schinkel, J.H. Beijnen,  
 620 Development and validation of a bioanalytical method for the quantification of the CDK4/6  
 621 inhibitors abemaciclib, palbociclib, and ribociclib in human and mouse matrices using liquid  
 622 chromatography-tandem mass spectrometry, *Anal. Bioanal. Chem.* 411 (2019) 5331–5345.  
 623 <https://doi.org/10.1007/s00216-019-01932-w>.
- 624 [33] J. Jolibois, A. Schmitt, B. Royer, A simple and fast LC-MS/MS method for the routine  
 625 measurement of cabozantinib, olaparib, palbociclib, pazopanib, sorafenib, sunitinib and its  
 626 main active metabolite in human plasma, *J. Chromatogr. B Analyt. Technol. Biomed. Life. Sci.*  
 627 1132 (2019) 121844. <https://doi.org/10.1016/j.jchromb.2019.121844>.
- 628 [34] B. Posocco, M. Buzzo, A.S. Poetto, M. Orleni, S. Gagno, M. Zanchetta, V. Iacuzzi, M.  
 629 Guardascione, F. Puglisi, D. Basile, G. Pelizzari, E. Marangon, G. Toffoli, Simultaneous  
 630 quantification of palbociclib, ribociclib and letrozole in human plasma by a new LC-MS/MS  
 631 method for clinical application, *PLoS One.* 15 (2020) e0228822.  
 632 <https://doi.org/10.1371/journal.pone.0228822>.
- 633 [35] F. Leenhardt, M. Gracia, C. Perrin, C. Muracciole-Bich, B. Marion, C. Roques, M. Alexandre, N.  
 634 Firmin, S. Poudroux, L. Mbatchi, C. Gongora, W. Jacot, A. Evrard, Liquid chromatography-  
 635 tandem mass spectrometric assay for the quantification of CDK4/6 inhibitors in human plasma  
 636 in a clinical context of drug-drug interaction, *J. Pharm. Biomed. Anal.* (2020) 113438.  
 637 <https://doi.org/10.1016/j.jpba.2020.113438>.
- 638





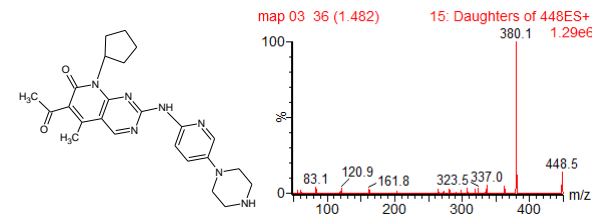
**Cobimetinib**

Molecular Formula:  $C_{22}H_{25}F_3IN_3O$   
 Formula Weight: 531.3530796  
 [M+H]<sup>+</sup>: 532.106708 Da



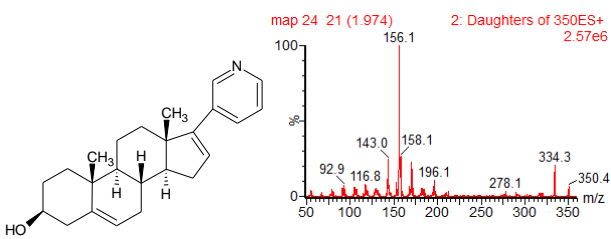
**Vemurafenib**

Molecular Formula:  $C_{23}H_{18}ClF_2N_3O_3S$   
 Formula Weight: 489.9221264  
 [M+H]<sup>+</sup>: 490.079822 Da



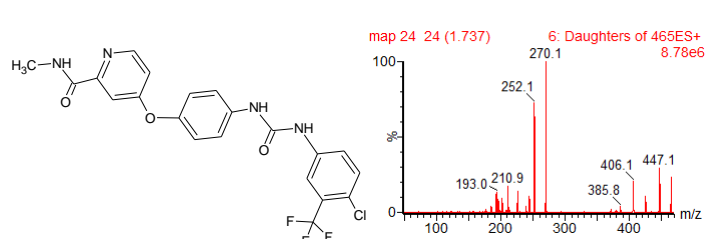
**Palbociclib**

Molecular Formula:  $C_{24}H_{29}N_7O_2$   
 Formula Weight: 447.53276  
 [M+H]<sup>+</sup>: 448.24555 Da



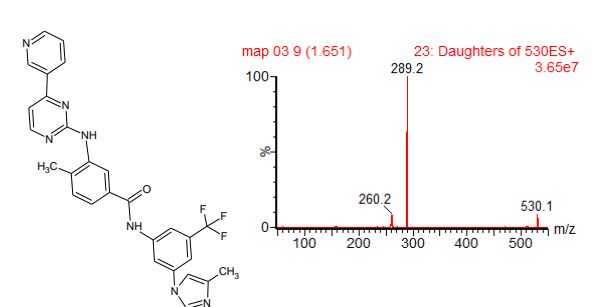
**Abiraterone**

Molecular Formula:  $C_{24}H_{31}NO$   
 Formula Weight: 349.50904  
 [M+H]<sup>+</sup>: 350.247841 Da



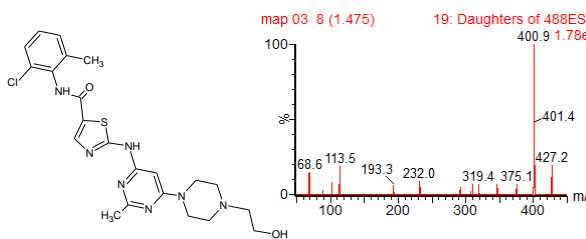
**Sorafenib**

Molecular Formula:  $C_{21}H_{16}ClF_2N_3O_3$   
 Formula Weight: 464.8249496  
 [M+H]<sup>+</sup>: 465.093579 Da



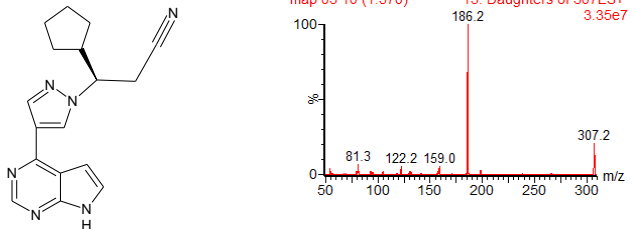
**Nilotinib**

Molecular Formula:  $C_{28}H_{22}F_3N_7O$   
 Formula Weight: 529.5157896  
 [M+H]<sup>+</sup>: 530.191069 Da



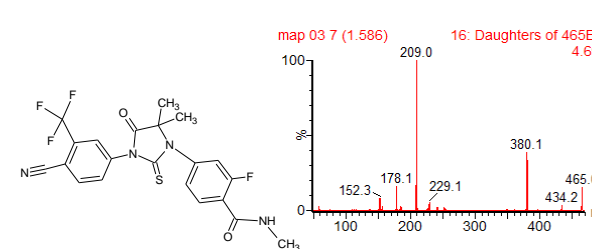
**Dasatinib**

Molecular Formula:  $C_{22}H_{26}ClN_4O_2S$   
 Formula Weight: 488.00554  
 [M+H]<sup>+</sup>: 488.162997 Da



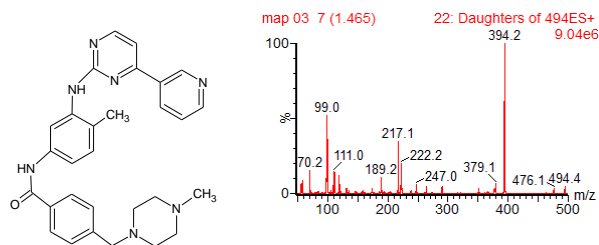
**Ruxolitinib**

Molecular Formula:  $C_{17}H_{18}N_6$   
 Formula Weight: 306.36502  
 [M+H]<sup>+</sup>: 307.166571 Da



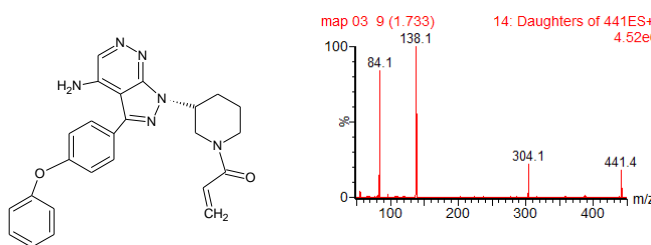
**Enzalutamide**

Molecular Formula:  $C_{21}H_{16}F_4N_4O_2S$   
 Formula Weight: 464.4359528  
 [M+H]<sup>+</sup>: 465.100285 Da



**Imatinib**

Molecular Formula:  $C_{29}H_{31}N_7O$   
 Formula Weight: 493.60274  
 [M+H]<sup>+</sup>: 494.266285 Da



**Ibrutinib**

Molecular Formula:  $C_{25}H_{24}N_6O_2$   
 Formula Weight: 440.49706  
 [M+H]<sup>+</sup>: 441.20335 Da

**Figure 1. Chemical structures of analytes and theoretical characteristics relevant to their detection by mass spectrometry.**

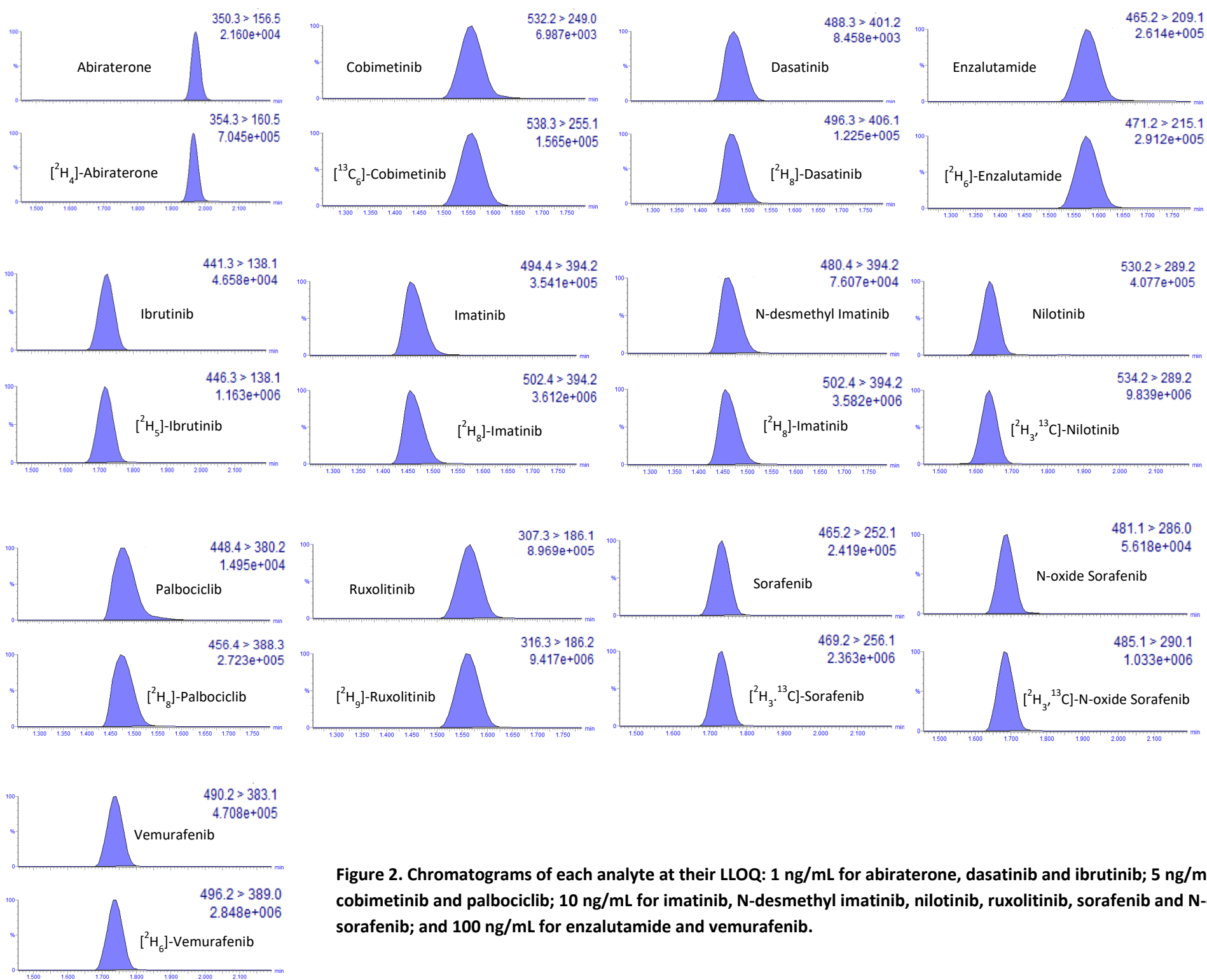
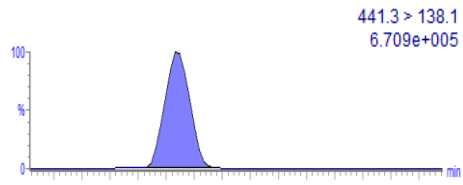
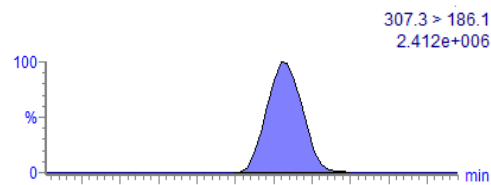


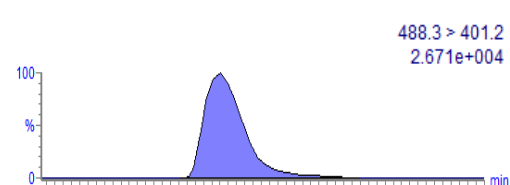
**Figure 2. Chromatograms of each analyte at their LLOQ: 1 ng/mL for abiraterone, dasatinib and ibrutinib; 5 ng/mL for cobimetinib and palbociclib; 10 ng/mL for imatinib, N-desmethyl imatinib, nilotinib, ruxolitinib, sorafenib and N-oxide sorafenib; and 100 ng/mL for enzalutamide and vemurafenib.**



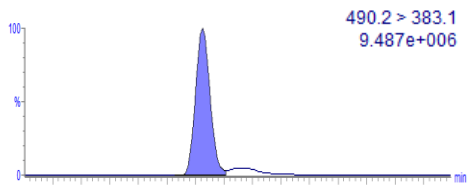
Ibrutinib (280 mg QD)  
C<sub>trough</sub> = 27.6 ng/mL



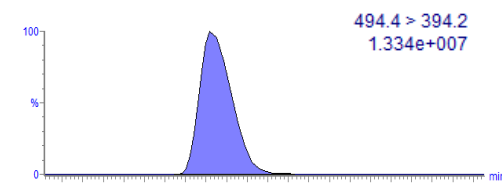
Ruxolitinib (20 mg BID)  
C<sub>trough</sub> = 82.7 ng/mL



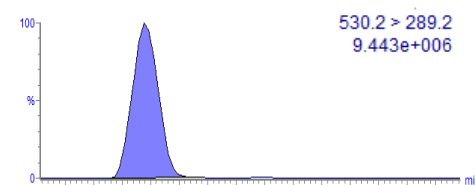
Dasatinib (100 mg QD)  
C<sub>max</sub> = 15.7 ng/mL



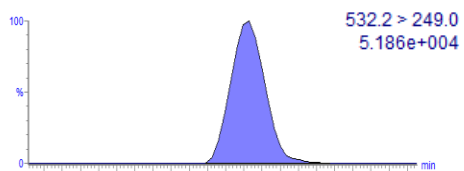
Vemurafenib (240 mg QD)  
C<sub>trough</sub> = 10,947 ng/mL



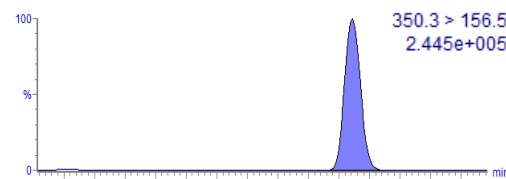
Imatinib (400 mg QD)  
C<sub>trough</sub> = 2,024 ng/mL



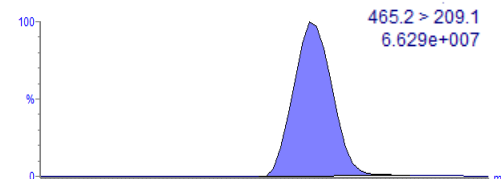
Nilotinib (300 mg BID)  
C<sub>trough</sub> = 960.2 ng/mL



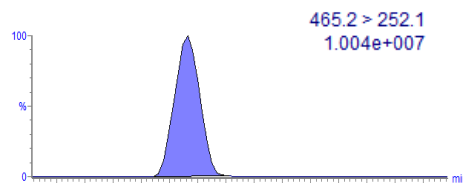
Cobimetinib (40 mg QD)  
C<sub>trough</sub> = 12.5 ng/mL



Abiraterone (1,000 mg QD)  
C<sub>trough</sub> = 15.6 ng/mL



Enzalutamide (160 mg QD)  
C<sub>trough</sub> = 16,770 ng/mL



Sorafenib (400 mg BID)  
C<sub>trough</sub> = 4,699 ng/mL

**Figure 3. Typical chromatograms of the targeted therapies obtained in plasma of patients.**

**Table 1. Pharmacological characteristics of oral targeted therapies analysed in this study (data from summary of products characteristics)**

Drug (INN)	Targets	Cancer indication	Metabolic pathway	Food effect AUC	Inhibitors effect CYP 3A4	Inductors effect CYP 3A4
Abiraterone acetate	CYP 17A1	Prostate	CYP 3A4	x 10	/	-55% AUC
Cobimetinib	MEK	Melanoma	CYP 3A4/5 UGT 2B7	/	Increase AUC	Decrease AUC
Dasatinib	Bcr-Abl, Src, c-Kit, PDGFR, EphR	CML, ALL Phi+	CYP 3A4	+14%	4 x Cmax 5 x AUC	-81% Cmax -82% AUC
Enzalutamide	Androgen receptors	Prostate	CYP 2C8 CYP 3A4/5	/	+41 to +326% AUC	-37% AUC
Ibrutinib	BTK	Mantel cell lymphoma, CLL	CYP 3A4	+160%	29 x Cmax 24 x AUC	-90% Cmax and AUC
Imatinib	Bcr-Abl, PDGFR, c-Kit	CML, ALL Phi+, GIST	CYP 3A4	-11%	+26% Cmax +40% AUC	-54% Cmax -74% AUC
Nilotinib	Bcr-Abl, PDGFR, c-Kit	CML	CYP 3A4	+29 to 82%	1,8 x Cmax 3 x AUC	-64% Cmax -80% AUC
Palbociclib	CDK4/6	Breast (HR+, HER2-) with concomittant hormone therapy	CYP 3A4 SULT 2A1	+12 to +21%	+34% Cmax +87% AUC	-70% Cmax -85% AUC
Ruxolitinib	JAK1/JAK2	myelofibrosis, GVH	CYP 3A4 CYP 2C9	/	+33 to +47% Cmax +91 to +232% AUC	-70% AUC
Sorafenib	VEGFR, PDGFR, B-Raf, C-Raf, c-Kit, Fit-3, MEK	Hepatocellular carcinoma, thyroid, renal	CYP 3A4 UGT	-29 to +14%	/	-37% AUC
Vemurafenib	B-Raf (V600E)	Melanoma, Erdheim-chester disease	CYP 3A4	+200%	Increase Cmax and AUC	Decrease Cmax and AUC

ALL: acute lymphoblastic leukemia, AUC: area under the curve, Bcr-Abl: breakpoint cluster region-Abelson complex, B-Raf: serine/threonine-protein kinase B-Raf, BTK: Burton tyrosine kinase, CDK4/6: cyclin-dependent kinase 4/6, c-Kit: tyrosine-protein kinase Kit, CLL: chronic lymphocytic leukemia, CML: chronic myeloid leukemia, C-Raf: serine/threonine-protein kinase C-Raf, CYP 17A1: 17 $\alpha$ -hydroxylase/C17,20-lyase, CYP 3A4: cytochrome P450 3A4, EphR: erythropoietin-producing human hepatocellular receptor, GIST: Gastrointestinal stromal tumours, GVH: graft versus host disease, HER2: human epidermal growth factor receptor, HR: hormonal receptor, JAK1/JAK2: janus kinase 1 and 2, MEK: mitogen-activated protein kinase, PDGFR: platelet-derived growth factor receptor, Src: tyrosine-protein kinase Src, SULT: Sulfotransferase, UGT: UDP-glycosyltransferase, VEGFR: vascular endothelial growth factor receptor.

**Table 2. Calibration range, linear regression equation, correlation coefficient, retention time, MRM transition, collision energie, cone potential and dwell time for each tested analyte.**

Analyte	Calibration Range (ng/mL)	Calibration curve Linear regression Equation	Coefficient of Correlation (r)	Retention Time (min)	MRM-Transition (m/z)	Collision Energie (V)	Cone Potential (V)	Dwell Time (s)
Abiraterone	1-500	$y = 0.0138x - 0.0072$	0.9995	1.97	350.3 > 156.5	50	60	0.005
Cobimetinib	5-500	$y = 0.0216x - 0.0012$	0.9999	1.56	532.2 > 249.0	35	50	0.005
Dasatinib	1-500	$y = 0.0305x + 0.0130$	0.9990	1.47	488.3 > 401.0	30	60	0.005
Enzalutamide	100-50,000	$y = 0.0002x + 0.0079$	0.9988	1.57	465.2 > 209.1	25	50	0.005
Ibrutinib	1-500	$y = 0.0145x + 0.0234$	0.9988	1.71	441.3 > 138.1	25	60	0.005
Imatinib	10-5,000	$y = 0.0018x - 0.0028$	0.9999	1.46	494.4 > 394.2	25	60	0.005
N-desmethyl Imatinib	10-5,000	$y = 0.0005x + 0.0040$	0.9972	1.46	480.4 > 394.2	30	40	0.005
Nilotinib	10-5,000	$y = 0.0016x - 0.0012$	0.9999	1.64	530.2 > 289.2	30	60	0.005
N-oxide Sorafenib	10-5,000	$y = 0.0020x - 0.0056$	0.9997	1.68	481.1 > 286.0	25	50	0.005
Palbociclib	5-500	$y = 0.0204x - 0.0240$	0.9997	1.48	448.4 > 380.2	28	50	0.005
Ruxolitinib	10-5,000	$y = 0.0035x + 0.0046$	0.9993	1.57	307.3 > 186.1	25	50	0.005
Sorafenib	10-5,000	$y = 0.0039x - 0.0068$	0.9999	1.73	465.2 > 252.1	30	50	0.005
Vemurafenib	100-100,000	$y = 0.0007x - 0.0123$	0.9998	1.74	490.2 > 383.1	26	45	0.005
[ <sup>2</sup> H <sub>4</sub> ]-Abiraterone	/	/	/	1.96	354.3 > 160.5	50	60	0.005
[ <sup>13</sup> C <sub>6</sub> ]-Cobimetinib	/	/	/	1.55	538.3 > 255.1	35	45	0.005
[ <sup>2</sup> H <sub>8</sub> ]-Dasatinib	/	/	/	1.46	496.3 > 406.1	30	60	0.005
[ <sup>2</sup> H <sub>6</sub> ]-Enzalutamide	/	/	/	1.57	471.2 > 215.1	25	50	0.005
[ <sup>2</sup> H <sub>5</sub> ]-Ibrutinib	/	/	/	1.72	446.3 > 138.1	25	60	0.005
[ <sup>2</sup> H <sub>8</sub> ]-Imatinib	/	/	/	1.45	502.4 > 394.2	25	55	0.005
[ <sup>2</sup> H <sub>3</sub> , <sup>13</sup> C]-Nilotinib	/	/	/	1.63	534.2 > 289.2	30	60	0.005
[ <sup>2</sup> H <sub>3</sub> , <sup>13</sup> C]-N-oxide Sorafenib	/	/	/	1.68	485.1 > 290.1	25	60	0.005
[ <sup>2</sup> H <sub>8</sub> ]-Palbociclib	/	/	/	1.47	456.4 > 388.3	28	50	0.005
[ <sup>2</sup> H <sub>9</sub> ]-Ruxolitinib	/	/	/	1.56	316.3 > 186.2	25	50	0.005
[ <sup>2</sup> H <sub>3</sub> , <sup>13</sup> C]-Sorafenib	/	/	/	1.73	469.2 > 256.1	30	50	0.005
[ <sup>2</sup> H <sub>6</sub> ]-Vemurafenib	/	/	/	1.73	496.2 > 389.1	26	45	0.005

**Table 3. Assay precision. Data detailing intra-day precision (n = 6) and inter-day precision (n = 6/day; 3 days : n = 18) of each analyte in human plasma.**

Analyte	Precision (% CV)							
	LLOQ		LQC		MQC		HQC	
	Intra-day	Inter-day	Intra-day	Inter-day	Intra-day	Inter-day	Intra-day	Inter-day
Abiraterone	9.9	11.8	2.6	5.5	1.9	2.1	2.5	2.3
Cobimetinib	9.2	14.7	7.2	8.9	2.9	3.3	3.4	4.3
Dasatinib	11.3	19.2	6.8	8.2	4.0	5.2	4.1	4.9
Enzalutamide	8.4	10	8.3	9.3	7.2	7.6	5.7	6.5
Ibrutinib	11.4	14.8	2.4	2.5	1.1	7.0	9.4	11.3
Imatinib	3.1	2.9	2.0	2.8	0.8	1.7	1.5	3.2
N-desmethyl Imatinib	7.8	13.8	4.5	5.6	2.6	5.2	2.8	4.4
Nilotinib	5.2	6.4	1.6	1.7	0.9	1.5	0.9	1.4
N-oxide Sorafenib	6.5	7.2	3.5	3.8	1.6	3.2	1.8	3.1
Palbociclib	5.9	6.3	4.3	7.3	3.2	5.1	2.3	3.8
Ruxolitinib	2.9	7.8	1.6	3.1	0.9	1.5	1.1	1.6
Sorafenib	4.2	11.2	2.5	2.4	5.4	5.9	8.5	9.7
Vemurafenib	3.6	6.4	2.1	3.7	2.7	12.3	4.5	9.8

CV: coefficient of variation

**Table 4. Assay accuracy. Data detailing inter-day accuracy (n = 6/day; 3 days: n = 18) of each analyte in human plasma.**

Analyte	Concentration (ng/mL)											
	LLOQ			LQC			MQC			HQC		
	Nominal	Mean Measured ± SD	Accuracy (% true)	Nominal	Mean Measured ± SD	Accuracy (% true)	Nominal	Mean Measured ± SD	Accuracy (% true)	Nominal	Mean Measured ± SD	Accuracy (% true)
Abiraterone	1	1.15 ± 0.14	115	10	10.4 ± 0.6	104	100	96 ± 2	96	400	408 ± 9	102
Cobimetinib	5	4.9 ± 0.7	98	10	9.4 ± 0.8	94	100	92 ± 3	92	400	381 ± 16	95
Dasatinib	1	1.02 ± 0.20	102	10	9.9 ± 0.8	99	100	92 ± 5	92	400	383 ± 19	96
Enzalutamide	100	114 ± 11	114	1,000	1,010 ± 94	101	10,000	9,260 ± 704	93	40,000	39,200 ± 2,548	98
Ibrutinib	1	0.95 ± 0.14	95	10	9.9 ± 0.2	100	100	96 ± 7	96	400	395 ± 45	99
Imatinib	10	11.4 ± 0.3	114	100	98 ± 3	98	1,000	975 ± 17	98	4,000	3,945 ± 126	99
N-desmethyl Imatinib	10	9.5 ± 1.3	95	100	110 ± 6	110	1,000	1,090 ± 57	109	4,000	4,033 ± 177	101
Nilotinib	10	11.2 ± 0.7	112	100	108 ± 2	108	1,000	1,084 ± 16	108	4,000	4,390 ± 61	110
N-oxide Sorafenib	10	11.0 ± 0.8	110	100	102 ± 4	103	1,000	1,030 ± 33	103	4,000	4,157 ± 129	104
Palbociclib	5	5.5 ± 0.3	109	10	9.4 ± 0.7	94	100	89 ± 5	89	400	388 ± 15	97
Ruxolitinib	10	9.9 ± 0.8	100	100	105 ± 3	105	1,000	1,062 ± 16	106	4,000	4,220 ± 68	106
Sorafenib	10	9.3 ± 1.0	93	100	94 ± 2	94	1,000	973 ± 57	97	4,000	3,712 ± 360	93
Vemurafenib	100	107 ± 7	107	1,000	960 ± 36	96	10,000	8,900 ± 1,095	89	80,000	74,400 ± 7,291	93

SD: standard deviation

**Table 5. Matrix effect (ME), extraction recovery (ER) and stability of each analyte at LQC, MQC and HQC in human plasma (n = 5)**

Analyte	QC level	ME (%) + CV (%)	ER (%) + CV (%)	Stability: % true + CV (%)			
				25°C for 72h	4°C for 1 week	-20°C for 8 weeks	3 freeze/thaw cycles
Abiraterone	LQC	88 + 6.4	77 + 5.9	108 + 6.6	108 + 5.3	104 + 4.2	111 + 7.6
	MQC	90 + 10.8	76 + 9.7	97 + 1.3	100 + 3.5	100 + 2.1	103 + 10.4
	HQC	87 + 9.9	82 + 9.9	97 + 2.2	107 + 4.4	104 + 1.3	97 + 4.4
Cobimetinib	LQC	113 + 7.2	111 + 2.1	92 + 4.9	102 + 12.7	103 + 2.8	99 + 6.7
	MQC	115 + 2.0	103 + 3.8	97 + 3.3	104 + 4.2	98 + 3.6	103 + 3.2
	HQC	112 + 4.3	105 + 1.3	100 + 2.8	105 + 3.6	101 + 1.9	96 + 0.9
Dasatinib	LQC	92 + 12.2	103 + 11.6	94 + 5.8	109 + 3.8	94 + 6.3	91 + 4.7
	MQC	95 + 4.2	99 + 7.9	95 + 5.7	102 + 8.1	98 + 2.3	96 + 2.6
	HQC	96 + 3.0	111 + 0.9	99 + 5.8	99 + 7.5	99 + 1.2	95 + 5.7
Enzalutamide	LQC	100 + 12.3	98 + 12.4	96 + 9.7	103 + 11.3	92 + 10.8	104 + 11.3
	MQC	98 + 5.9	102 + 2.4	94 + 11.1	104 + 1.5	92 + 2.9	108 + 3.8
	HQC	101 + 5.4	103 + 3.3	104 + 9.6	103 + 6.0	94 + 1.2	107 + 3.9
Ibrutinib	LQC	92 + 13.1	107 + 11.5	65 + 7.5	72 + 8.5	90 + 5.0	107 + 4.9
	MQC	109 + 11.7	104 + 9.8	68 + 3.3	76 + 2.9	108 + 2.2	99 + 6.6
	HQC	105 + 2.9	101 + 0.8	74 + 10.0	80 + 10.4	107 + 2.4	95 + 10.5
Imatinib	LQC	101 + 2.7	99 + 4.1	96 + 3.0	99 + 3.6	99 + 0.8	88 + 1.8
	MQC	92 + 1.2	100 + 1.5	96 + 1.5	99 + 1.5	98 + 1.6	90 + 0.7
	HQC	98 + 4.0	111 + 1.7	97 + 0.5	99 + 1.9	100 + 1.2	89 + 2.7
N-desmethyl Imatinib	LQC	117 + 3.1	95 + 3.7	94 + 2.2	93 + 3.1	91 + 1.5	94 + 2.1
	MQC	104 + 1.3	102 + 2.3	101 + 3.5	97 + 1.7	99 + 3.3	93 + 3.2
	HQC	114 + 4.4	109 + 1.4	104 + 1.5	98 + 5.2	101 + 2.0	96 + 4.3
Nilotinib	LQC	92 + 6.3	105 + 5.8	97 + 2.4	99 + 5.0	102 + 1.4	107 + 1.4
	MQC	98 + 5.8	94 + 7.3	94 + 0.6	96 + 1.6	100 + 0.7	101 + 2.6
	HQC	103 + 3.3	97 + 4.2	97 + 1.1	95 + 2.3	100 + 0.4	100 + 0.6
N-oxide Sorafenib	LQC	97 + 11.7	107 + 6.8	101 + 1.8	97 + 6.1	96 + 4.8	112 + 5.1
	MQC	94 + 4.4	102 + 0.8	94 + 1.3	96 + 3.7	97 + 2.4	102 + 4.8
	HQC	102 + 2.9	110 + 6.1	98 + 1.0	98 + 2.8	97 + 1.2	101 + 2.1
Palbociclib	LQC	122 + 11.5	113 + 2.0	94 + 6.1	108 + 2.3	95 + 4.6	103 + 9.7
	MQC	92 + 2.9	108 + 2.1	95 + 2.2	105 + 3.2	94 + 2.7	96 + 2.6
	HQC	95 + 3.6	111 + 6.1	96 + 1.6	100 + 5.9	98 + 0.9	97 + 5.6
Ruxolitinib	LQC	98 + 8.8	108 + 2.7	97 + 0.5	98 + 3.3	96 + 1.5	98 + 2.2
	MQC	95 + 6.9	101 + 1.0	97 + 0.9	99 + 2.3	102 + 1.3	99 + 2.4
	HQC	101 + 3.3	101 + 3.2	99 + 1.1	101 + 3.1	101 + 1.4	101 + 2.7
Sorafenib	LQC	98 + 12.8	92 + 9.7	100 + 2.0	101 + 6.1	95 + 1.1	112 + 3.6
	MQC	90 + 10.9	94 + 4.3	96 + 0.8	105 + 2.0	99 + 1.6	98 + 9.6
	HQC	92 + 9.8	104 + 6.2	91 + 0.9	106 + 3.1	98 + 1.8	98 + 4.9
Vemurafenib	LQC	107 + 4.7	100 + 3.4	101 + 4.5	98 + 3.4	103 + 1.9	102 + 2.0
	MQC	99 + 6.4	92 + 1.3	92 + 1.1	98 + 1.6	98 + 1.5	108 + 2.7
	HQC	103 + 3.9	98 + 1.5	95 + 0.7	99 + 2.9	94 + 2.2	106 + 1.8

CV: coefficient of variation. n: number of replicates



**Table 6. Results of the samples of patients treated with oral targeted therapies.**

Drug (INN)	Number of patients	Dose (mg)	Steady-state C <sub>trough</sub> † (ng/mL)	C <sub>max</sub> ‡ (ng/mL)	AUC <sub>0-24h</sub> § (ng.h <sup>-1</sup> .mL <sup>-1</sup> )	Established or accepted target concentration Ref [7]
Abiraterone	7	1,000 mg QD	12.0 [3.1-16.3]*	/	/	C <sub>trough</sub> > 8.4 ng/mL
Cobimetinib	19	20 [20-40]* mg QD	54.0 [6.5-227.8]*	/	/	C <sub>trough</sub> : 75-290 ng/mL**
Dasatinib	2	100 mg QD	2.1 ; 4.7	15.7 ; 28.3	/	C <sub>trough</sub> : 1.4-3.4 ng/mL; C <sub>max</sub> > 50 ng/mL
Enzalutamide	4	160 mg QD	13,322 [9,240-16,770]*	/	/	C <sub>trough</sub> > 10,000 ng/mL
Ibrutinib	15	420 [140-560]* mg QD	5.5 [1.2-80.1]*	113.1 [6.4-355.5]*	918 [69-3,210]*	C <sub>max</sub> < 170 ng/mL, AUC: 680 ± 517 ng.h <sup>-1</sup> .mL <sup>-1</sup>
Imatinib	4	400 mg QD	805.1 [141.8-2,024]*	/	/	C <sub>trough</sub> > 1,000 ng/mL
N-desmethyl Imatinib	/	/	213.1 [97.2-432.7]*	/	/	/
Nilotinib	2	300 mg BID	960.2 ; 1,601	/	/	C <sub>trough</sub> : 480-1,580 ng/mL
Ruxolitinib	5	15 [15-20]* mg BID	37.3 [11.7-82.7]*	162.4 [139.8-204.2]*	/	C <sub>trough</sub> : 5.4-17.4 ng/mL; C <sub>max</sub> : 140-277 ng/mL
Sorafenib	7	400 [200-400]* mg BID	4,242 [3,475-5,684]*	/	/	C <sub>trough</sub> : 3,750-4,300 ng/mL
N-oxide Sorafenib	/	/	432.3 [142.7-941.4]*	/	/	/
Vemurafenib	15	240 [240-960]* mg BID	16,654 [7,583-67,774]*	/	/	C <sub>trough</sub> > 40,000 ng/mL**

\* Median [min-max], QD: once a day, BID: two times a day

\*\* Therapeutic range in melanoma. No data in erdheim-chester disease

† For all patients, the samples were taken at least 5 days after the start of treatment or change in dose

‡ C<sub>max</sub> was measured at T1h, T2h and T3h after taking the drug for ruxolitinib, ibrutinib and dasatinib, respectively

§ AUC<sub>0-24h</sub> was estimated using 3 successive samples at T0, T2h and T4h by noncompartmental method using WinNonLin® software